The brighter galaxies reionized the Universe

Mahavir Sharma,[1]⋆ Tom Theuns,[1]⋆ Carlos Frenk,[1] Richard Bower,[1] Robert Crain,[2] Matthieu Schaller[1] and Joop Schaye[3]

[1]*Department of Physics, Institute for Computational Cosmology, University of Durham, South Road, Durham DH1 3LE, UK*
[2]*Astrophysics Research Institute, Liverpool John Moores University, 146 Brownlow Hill, Liverpool L3 5RF, UK*
[3]*Leiden Observatory, Leiden University, PO Box 9513, NL-2300 RA Leiden, the Netherlands*

ABSTRACT

Hydrogen in the Universe was (re)ionized between redshifts $z \approx 10$ and $z \approx 6$. The nature of the sources of the ionizing radiation is hotly debated, with faint galaxies below current detection limits regarded as prime candidates. Here, we consider a scenario in which ionizing photons escape through channels punctured in the interstellar medium by outflows powered by starbursts. We take account of the observation that strong outflows occur only when the star formation density is sufficiently high, and estimate the galaxy-averaged escape fraction as a function of redshift and luminosity from the resolved star formation surface densities in the EAGLE cosmological hydrodynamical simulation. We find that the fraction of ionizing photons that escape from galaxies increases rapidly with redshift, reaching values of 5–20 per cent at $z > 6$, with the brighter galaxies having higher escape fractions. Combining the dependence of escape fraction on luminosity and redshift with the observed luminosity function, we demonstrate that galaxies emit enough ionizing photons to match the existing constraints on reionization while also matching the observed ultraviolet-background post-reionization. Our findings suggest that galaxies above the current *Hubble Space Telescope* detection limit emit half of the ionizing radiation required to reionize the Universe.

Key words: galaxies: starburst – dark ages, reionization, first stars.

1 INTRODUCTION

Consensus is emerging that neutral hydrogen in the Universe was (re)ionized between redshifts $z \approx 10$ and $z \approx 6$ (e.g. McGreer, Mesinger & D'Odorico 2015; Mitra, Choudhury & Ferrara 2015; Robertson et al. 2015). The nature of the sources of the ionizing radiation has not yet been firmly established, but attention has focused on an early generation of galaxies. Regions around such galaxies are ionized first, and these ionized bubbles grow in number and size until they percolate as more and brighter galaxies form (Gnedin 2000; Shin, Trac & Cen 2008). Therefore, as reionization proceeds, a larger fraction of the Universe becomes ionized (see e.g. Loeb & Barkana 2001 for a review).

A crucial factor in modelling reionization is the fraction of ionizing photons that escape their natal galaxy, f_{esc}. Neutral hydrogen and dust in the interstellar medium (ISM) and circumgalactic medium (CGM) determine a galaxy's f_{esc}. This quantity is difficult to measure and observational claims of the detection of ionizing photons escaping from galaxies are controversial. The value of f_{esc} is often assumed to be constant (e.g. Bouwens et al. 2011; Robertson

et al. 2013) or increasing towards lower luminosities (e.g. Ferrara & Loeb 2013). In such models, faint galaxies far below current detection limits dominate the ionizing emissivity.

Observed values of f_{esc} at $z \approx 0$ are generally a few per cent or less. For example, Bland-Hawthorn & Maloney (2001) infer a value of $f_{esc} \approx 1$–2 per cent for the Milky Way galaxy. Such low values are not surprising since star-forming regions are usually enshrouded in neutral gas with column density $N_{HI} \gtrsim 10^{20}$ cm^{-2}, three orders of magnitude higher than the value that yields an optical depth of $\tau = 1$ for ionizing photons with energy 1 Rydberg; it is this neutral gas that fuels star formation in the first place. For galaxies to be able to reionize the Universe by $z \approx 6$ and provide the bulk of the ionizing photons post-reionization, f_{esc} needs to increase rapidly with redshift, $\propto (1 + z)^{3.4}$ according to Haardt & Madau (2012) or even faster (Khaire et al. 2015). Such a rapid evolution of the escape fraction then suggests that the ISM/CGM of high-z galaxies is fundamentally different from that at low z; the expected decrease in dust content is not enough to explain the trend. Why this should be so is a mystery whose resolution is key to understanding cosmological reionization.

Whether the escape fraction indeed evolves (rapidly) can in principle be tested directly by measuring f_{esc} as function of redshift. There are currently no direct detections of ionizing photons escaping from individual galaxies at $z \approx 1$ (Bridge et al. 2010;

⋆ E-mail: mahavir.sharma@durham.ac.uk (MS); tom.theuns@durham.ac.uk (TT)

Siana et al. 2010; Rutkowski et al. 2015), with 3σ upper limits of $f_{esc} \approx 2$ per cent. In contrast, Nestor et al. (2013) measure $f_{esc} = 5$–7 per cent for $z \approx 3$ Lyman-break galaxies (see also Vanzella et al. 2012) and even higher values for Lyman-α emitters. These values are significantly higher than more recent determination of a value <2 per cent by Grazian et al. (2015) for LBGs at $3.3 < z < 4$. The observational evidence for evolution in f_{esc} is thus currently inconclusive.

Numerical simulations of galaxy formation that include radiative transfer, aimed at calculating f_{esc} at $z \gtrsim 6$, also yield contradictory results. Kimm & Cen (2014) quote values of $f_{esc} \approx 10$ per cent, with even higher values of ≈ 20 per cent during starbursts. Paardekooper, Khochfar & Dalla Vecchia (2015) find much lower values, and claim that f_{esc} decreases rapidly with halo mass and cosmic time (see also Razoumov & Sommer-Larsen 2010; Yajima, Choi & Nagamine 2011; Wise et al. 2014). In contrast, Ma et al. (2015) find intermediate values, $f_{esc} \approx 5$ per cent, with no strong dependence on either galaxy mass or cosmic time. Most ionizing photons that do not make it out of their natal galaxy are absorbed locally – within several tens of parsecs of the star that emitted them. Consequently, the level of discrepancy between current simulations is not surprising, since the detailed properties of the ISM need to be modelled very accurately, with little guidance from observations.

A generic feature of these radiative transfer simulations is that starbursts clear channels in the ISM through which ionizing photons escape (e.g. Fujita et al. 2003), a phenomenon that is particularly efficient at $z \gtrsim 6$ when galaxies are particularly bursty (e.g. Wise & Abel 2008) and drive winds. Heckman (2001) uses X-ray and optical emission line data to conclude that winds occur in galaxies with star formation surface density above a critical value of $\dot{\Sigma}_{\star,crit} \approx 0.1$ $M_{\odot}$ yr^{-1} kpc^{-2}. Theoretical models of outflows driven by starbursts through supernovae (Clarke & Oey 2002), radiation pressure (Murray, Ménard & Thompson 2011) or turbulent stirring (Scannapieco, Gray & Pan 2012), support the existence of such a threshold, at similar values of $\dot{\Sigma}_{\star,crit}$ as inferred from observations.

If the lifetime of massive stars is shorter than the time required to create channels in the ISM, then the fraction of all ionizing photons that escapes from a galaxy may be small, even though f_{esc} is high once the channels have been created (Kimm & Cen 2014). Compact starbursts may suffer less from such a time-scale mismatch. Indeed, a wind moving with speed $v \geq 100$ km s^{-1} can carve a 500 pc wide channel in a time ≤ 5 Myr, comparable to the typical lifetime of a massive star. The few observed cases with large emissivities indeed result from very compact starbursts. Borthakur et al. (2014) and Izotov et al. (2016) find $f_{esc} \approx 20$ and 8 per cent, respectively, in $z \approx 0.2$–0.3 compact starbursts; de Barros et al. (2016) find a relative escape fraction of 60 per cent in a $z \approx 3$ compact starburst, and there is tantalizing evidence that photons escape in channels (e.g. Chen, Prochaska & Gnedin 2007; Zastrow et al. 2013).

Here, we propose a model in which f_{esc} for a star-forming region depends on the local star formation surface density averaged on a scale of ≈ 1 kpc^2, $\dot{\Sigma}_{\star}$, motivated by the arguments presented above. We assume that when $\dot{\Sigma}_{\star} \geq \dot{\Sigma}_{\star,crit}$ the escape fraction, f_{esc}, is constant and equal to $f_{esc,max}$ due to self-regulation of star formation. We take $f_{esc,max} \approx 0.2$, roughly the observed upper limit, but explore how our results change if $f_{esc,max}$ is varied between 0.1 and 0.4. When $\dot{\Sigma}_{\star} < \dot{\Sigma}_{\star,crit}$, we take $f_{esc} = 0$. We use this *Ansatz* to derive f_{esc} for all galaxies in the EAGLE simulation (Crain et al. 2015; Schaye et al. 2015). We do not perform radiative transfer on EAGLE galaxies directly since these simulations do not have enough resolution to model the physics that generates outflow-driven channels.

In Section 2, we calculate how the escape fraction depends on luminosity and redshift, illustrate what this implies for reionization, the amplitude of the ionizing background below $z = 6$, and the nature of the galaxies that reionized the Universe. We summarize in Section 3.

2 ESCAPE OF IONIZING PHOTONS FROM GALAXIES

2.1 The evolution of the star formation surface density

The EAGLE hydrodynamical cosmological simulations (Crain et al. 2015; Schaye et al. 2015) use subgrid modules for star and black hole formation, and feedback from stars and active galactic nucleus. The star formation rate is calculated as function of pressure that ensures that galaxies follow the observed relation at $z = 0$ between gas surface density and $\dot{\Sigma}_{\star}$ from Kennicutt (1998), as described in Schaye & Dalla Vecchia (2008), and the model assumes that this relation does not evolve. The star formation rate is assumed to be zero below the metallicity dependent threshold of Schaye (2004). Gas particles are stochastically converted into star particles with a probability per unit time that depends on their star formation rate. The EAGLE suite includes models that vary in numerical resolution to test for convergence. Here, we use two models, Ref-L0100N1504 (linear size $L = 100$ Mpc, gas particle mass $m_g = 1.81 \times 10^6$ M$_{\odot}$) and the higher resolution model Recal-L0025N0752 ($L = 25$ Mpc, $m_g = 2.26 \times 10^5$ M$_{\odot}$).

We compute f_{esc} of a galaxy by calculating the escape fraction of all its individual star-forming regions, and weighting them by their star formation rate. For an individual region we take $f_{esc} = f_{esc,max}$ when $\dot{\Sigma}_{\star} \geq \dot{\Sigma}_{\star,crit}$ and zero otherwise. Galaxies in EAGLE are both more active (higher $\dot{M}_{\star}/M_{\star}$) and smaller at earlier times. As a consequence, an increasing fraction of star-forming regions have higher ISM pressure (see fig. 7 in Crain et al. 2015), which have higher $\dot{\Sigma}_{\star}$ according to the star formation prescription of Schaye & Dalla Vecchia (2008), and hence higher f_{esc} as well.

The local quantity $\dot{\Sigma}_{\star}$ cannot be compared directly to observations. We therefore compute $\dot{\Sigma}_{\star,0} \equiv \dot{M}_{\star}/(2\pi R_{\star}^2)$, where $\dot{M}_{\star}$ is the star formation rate of the galaxy and $R_{\star}$ its half-mass radius; $\dot{\Sigma}_{\star,0}$ is the central surface density of star formation if the disc is exponential. In EAGLE, $\dot{\Sigma}_{\star,0}$ increases with $\dot{M}_{\star}$ at given redshift, and with redshift at given $\dot{M}_{\star}$ (coloured bands in Fig. 1). For example, for a galaxy with $\dot{M}_{\star} = 1$ M$_{\odot}$ yr^{-1}, $\dot{\Sigma}_{\star,0} = 10^{-2}$ M$_{\odot}$ yr^{-1} kpc^{-2} at $z = 0$, but is more than a factor of 10 higher at $z = 8$. The histogram in Fig. 1 shows this more quantitatively.

Observed galaxies display a very similar dependence of $\dot{\Sigma}_{\star,0}$ on $\dot{M}_{\star}$ and z as EAGLE galaxies (Fig. 1, data points are $\dot{\Sigma}_{\star,0}$ as function of $\dot{M}_{\star}$ for observed galaxies, with colours depending on redshift in the same manner as the coloured bands representing EAGLE). That EAGLE reproduces these trends so well is consistent with the fact that the simulation reproduces separately the observed trend of increasing $\dot{M}_{\star}/M_{\star}$ with z (Furlong et al. 2015a), and of decreasing size with z (Furlong et al. 2015b).

The strong evolution of the surface density of star formation suggests that an increasingly large fraction of galaxies drive winds at early times: whereas at $z = 0$ most galaxies have $\dot{\Sigma}_{\star,0} \ll \dot{\Sigma}_{\star,crit}$ and hence are not expected to drive winds (these are located in the hashed region in Fig. 1), at $z \gtrsim 6$ most galaxies have $\dot{\Sigma}_{\star,0} \gtrsim \dot{\Sigma}_{\star,crit}$ and their star-forming regions are expected to drive outflows.

A consequence of the rapid increase of $\dot{\Sigma}_{\star,0}$ with z is that f_{esc} also increases rapidly with z, as shown in Fig. 2. Large values of f_{esc} are extremely rare at $z = 0$; at $z = 3$ only the very brightest galaxies have
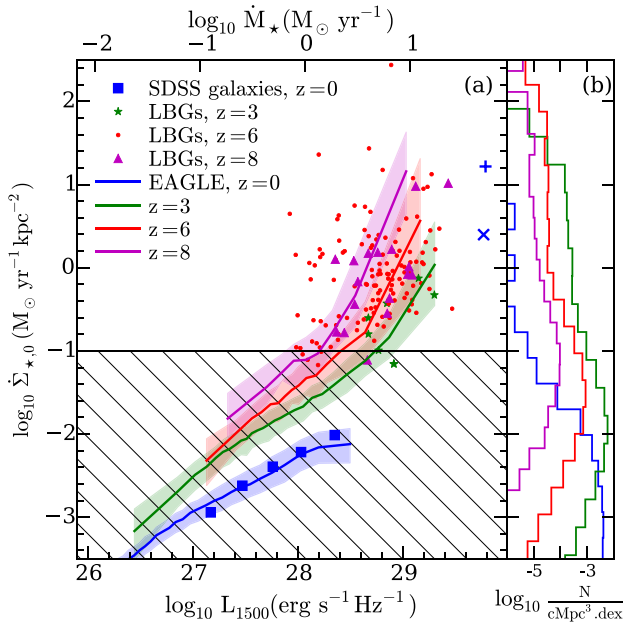
Figure 1. The dependence of the mean surface density of star formation, $\dot\Sigma_{\star,0}$, on star formation rate and redshift. Panel a: $\dot\Sigma_{\star,0}$ of EAGLE galaxies with stellar mass $>10^8\,\mathrm{M}_\odot$, as a function of their 1500 Å ultraviolet (UV) luminosity (L_{1500}, bottom axis, corresponding star formation rate, $\dot M_\star$, top axis), with coloured lines depicting the median relation, and coloured regions enclosing the 25th to 75th percentile range. Different colours refer to different redshifts (blue, $z=0$, green, $z=3$, red, $z=6$, magenta, $z=8$). $\dot\Sigma_{\star,0}$ increases with $\dot M_\star$ at given z, and with z at given $\dot M_\star$. Horizontal black line shows the critical star formation rate surface density ($\dot\Sigma_{\star,\mathrm{crit}}$) for outflows (Heckman 2001). Panel b: Number density of EAGLE galaxies in bins of $\dot\Sigma_{\star,0}$, using the same colour scheme. At $z=0$, galaxies with $\dot\Sigma_{\star,0}\gtrsim\dot\Sigma_{\star,\mathrm{crit}}$ above which significant winds develop are present in the simulation, but they are very rare. However at $z\gtrsim6$, most EAGLE galaxies with $\dot M_\star>1$ $\mathrm{M}_\odot\,\mathrm{yr}^{-1}$ are above this limit, and are expected to drive strong winds. Observed values of $\dot\Sigma_{\star,0}$ are plotted in panel a, with colours depending on z matching those of the simulation; the region of low $\dot\Sigma_{\star,0}$ where winds are not expected is hashed. The data shown are $z=0$, Sloan Digital Sky Survey measurements (Brisbin & Harwit 2012, squares), the galaxies with high values of f_{esc} from (Borthakur et al. 2014, cross) and (Izotov et al. 2016, plus), Lyman-break galaxies from Giavalisco, Steidel & Macchetto (1996) at $z=3$ (stars), from Curtis-Lake et al. (2016) at $z=6$ (small dots) and at $z=8$ (triangles). EAGLE galaxies reproduce the dependence of $\dot\Sigma_{\star,0}$ on $\dot M_\star$ and z.

significant non-zero values of $f_{\mathrm{esc}}\gtrsim10$ per cent (in the absence of dust); but above $z=6$ galaxies with $L_{1500}>10^{28}\,\mathrm{erg\,s}^{-1}\,\mathrm{Hz}^{-1}$ have a mean $f_{\mathrm{esc}}>10$ per cent, which increases further to $f_{\mathrm{esc}}>15$ per cent by $z=8$. There is good agreement (better than 10 per cent) in the predicted value of f_{esc} between models Ref-L0100N1504 and Recal-L0025N0752, that differ by a factor of 8 in mass resolution, for galaxies brighter than $10^{28}\,\mathrm{erg\,s}^{-1}\,\mathrm{Hz}^{-1}$. We use the higher resolution simulation to calculate f_{esc} for galaxies brighter than $10^{27}\,\mathrm{erg\,s}^{-1}\,\mathrm{Hz}^{-1}$.

Given the good agreement in the evolution of $\dot\Sigma_{\star,0}$ between EAGLE and observed galaxies, we conclude that the increased activity in galaxies, coupled with their smaller sizes, implies that f_{esc} increases rapidly with redshift in observed galaxies as well. Such vigorously star-forming galaxies are rare in the local Universe, but they do occur, both in the data and in the simulations which have a long tail to high $\dot\Sigma_{\star,0}$ as shown by the blue histogram in Fig. 1. In fact, the blue cross and plus symbols correspond to the low-z
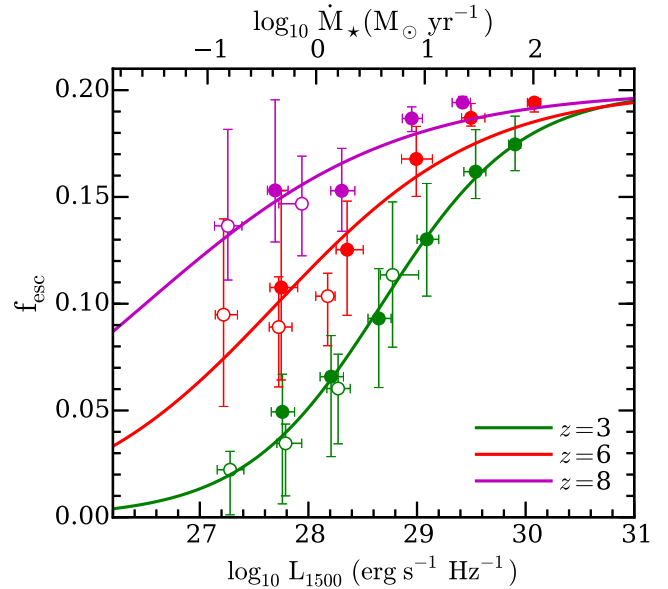

Figure 2. Mean inferred escape fraction for ionizing photons (f_{esc}) from galaxies in EAGLE as a function of the 1500 Å luminosity (L_{1500}) at three redshifts (green: $z=3$, red: $z=6$, magenta: $z=8$), for $f_{\mathrm{esc,\,max}}=0.2$. Circles represent the luminosity-weighted average of f_{esc}, with error bars encompassing the 25th to 75th percentile range. Filled circles refer to the reference simulation (labelled Ref-L0100N1504), open circles to the simulation that has eight times better mass resolution (labelled Recal-L0025N0752). Simulation results are fitted with a sigmoid function shown as solid curves. The escape fraction increases with luminosity and redshift.

galaxies identified by Borthakur et al. (2014) and Izotov et al. (2016) as having a high escape fraction corrected for dust of 20 and 8 per cent, respectively. (High-redshift star-forming galaxies show no evidence of the presence of dust, Bouwens et al. 2015a.) These are located in a similar region in the $\dot M_\star-\dot\Sigma_{\star,0}$ plot of Fig. 1 as most of the currently detected brighter galaxies at $z\gtrsim6$, and so we expect the latter to have similarly high values of f_{esc}. We investigate the consequences of a high escape fractions for galaxies with high values of $\dot\Sigma_\star$ next.

2.2 The contribution of observed galaxies to reionization

We can combine the dependence of the escape fraction on galaxy luminosity and redshift, $f_{\mathrm{esc}}(L_{1500},z)$, from Fig. 2 with the observed number density of galaxies as function of 1500 Å luminosity from Bouwens et al. (2015b), $\Phi(L_{1500})$, to obtain the emissivity at energies 13.6 eV, $\epsilon=f_{\mathrm{esc}}(L_\nu,z)\,\Phi(L_\nu,z)L(\nu_{\mathrm{th}},z)$, and the emissivity of ionizing photons, $\dot n_{\gamma,\mathrm{esc}}(L_{1500},z)=f_{\mathrm{esc}}(L_\nu,z)\,\Phi(L_\nu,z)\int_{\nu_{\mathrm{th}}}^\infty\frac{L_\nu}{h\nu}\,\mathrm{d}\nu$. Here, L_ν is the luminosity of the galaxy at a frequency ν and $h\nu_{\mathrm{th}}=13.6$ eV, the ionization potential of hydrogen. We use the luminosity function at 1500 Å from Bouwens et al. (2015b), and assume that the intrinsic spectrum of the ionizing sources has a break of $L(912\,\text{Å})/L(1500\,\text{Å})=1/6$ as in the STARBURST99 model[1] (Leitherer et al. 1999; Bruzual & Charlot 2003). Resulting values of ϵ and of the cumulative contribution to the emissivity of ionizing photons, $\dot n_{\gamma,\mathrm{esc}}(>L_{1500},z)$, are plotted in Fig. 3.

---

[1] We use the observed luminosity function without dust correction, implicitly assuming that dust obscuration affects ionizing and 1500 Å photons in the same way. The absolute escape fraction is then smaller than the values we quote by the (small) dust correction.
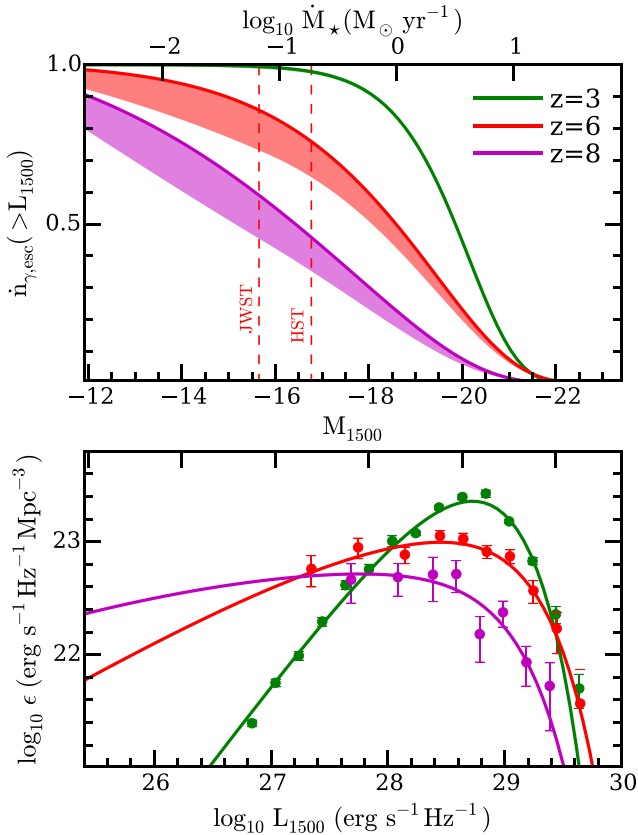
Figure 3. Detectability of the galaxies that reionized the Universe. Bottom panel: emissivity at 912 Å(ϵ) as a function of the 1500 Å luminosity of galaxies (middle axis shows corresponding M_{1500} magnitude on the AB-system, top axis the corresponding star formation rate) for redshifts $z = 3$ (green), 6 (red) and 8 (magenta). Curves combine the observed luminosity function of galaxies from Bouwens et al. (2015b) and Parsa et al. (2016), with model for the escape fraction of ionizing photons described in the text. Even though the galaxy luminosity functions steepen rapidly towards higher redshifts, brighter galaxies dominate the emissivity even at $z = 8$. Top panel: cumulative contribution of galaxies to the emissivity of ionizing photons ($\dot{n}_{\gamma,\mathrm{esc}}$) at the corresponding redshifts; the *HST* detection limit at $z = 6$ (Bouwens et al. 2015b) is shown as a red dashed line, the *JWST* detection limit for a 30 h integration is also indicated. The lower edge of the shaded region corresponds to using a constant value for f_{esc} for all galaxies fainter than $M_{1500} = -16$, and extrapolating the luminosity function to $M_{1500} = -10$.

At $z = 3$, the faint-end slope of the luminosity function is sufficiently flat that bright galaxies dominate both ϵ and the photon production rate. Interestingly, even though the luminosity function becomes much steeper at $z = 6$ and even more so at $z = 8$ (Bouwens et al. 2015b), bright galaxies still dominate at these earlier times, with 50 per cent of photons escaping from galaxies brighter than $M_{1500} = -18$ at $z = 6$, and $M_{1500} = -16.5$ at $z = 8$. This is because the escape fraction of galaxies drops with decreasing luminosity (Fig. 2) faster than that the number of such galaxies increases, even when luminosity function is very steep.

We show in Fig. 4 (bottom panel) that the evolution of the ionizing emissivity, $\dot{n}_{\gamma,\mathrm{esc}}$, is consistent with the latest constraints on reionization (Bouwens et al. 2015b, green band), and crucially, also with the emissivity required to produce the ionizing background post-reionization (Becker & Bolton 2013, blue band). In the top, we plot the cumulative fraction of ionizing photons emitted up to a
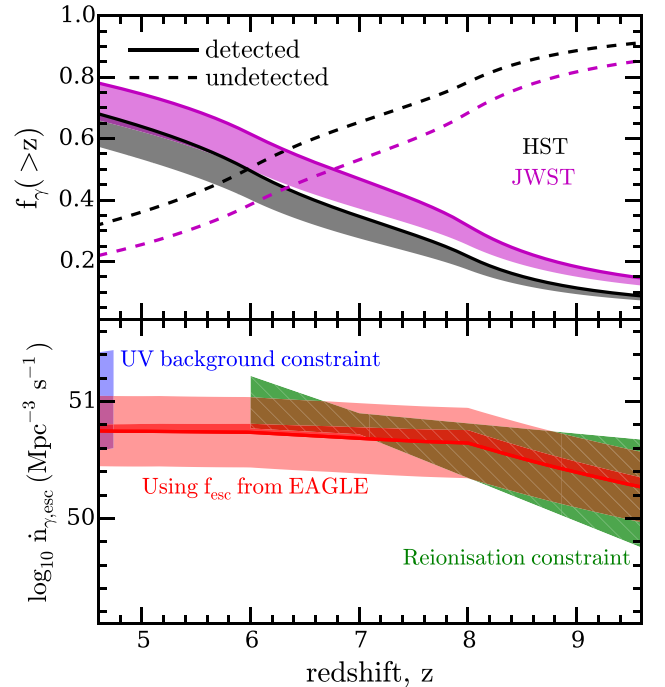
Figure 4. Total ionizing emissivity ($\dot{n}_{\gamma,\mathrm{esc}}$, bottom panel, solid red line) and fraction of that emissivity due to galaxies above a given detection limit ($f_{\gamma}(>z)$, top panel, *HST*: solid black; 30 h *JWST* limit: solid magenta), obtained by integrating the emissivity as function of luminosity from Fig. 3. Shaded region (dark shaded region in the lower panel) shows the range if a constant value for f_{esc} is used for galaxies fainter than $M_{1500} = -16$, and the luminosity function is extrapolated to $M_{1500} = -10$. The light red shaded region in the bottom panel, shows the range of emissivity when the maximum allowed escape fraction is varied between 10 and 40 per cent. The blue shaded region represents the range in $\dot{n}_{\gamma,\mathrm{esc}}$ required to match the amplitude of the UV-background (Becker & Bolton 2013); the green shaded region is the range required to match the Thomson optical depth and the evolution of the ionized volume fraction during reionization (Bouwens et al. 2015b). In our model, galaxies emit enough ionizing photons to match the reionization constraints as well as the lower-z amplitude of the UV-background. In this scenario, 50 per cent (60 per cent) of these photons are emitted by galaxies above the *HST* (*JWST*) limit by $z = 6$ (see top panel).

redshift z, $f_{\gamma}(>z)$, by the galaxies above the current detection limit of *Hubble Space Telescope* (*HST*) (black curve) and that predicted for a 30 h *James Webb Space Telescope* (*JWST*) integration (magenta curve). Before $z = 6$, approximately 50 per cent of the photons that reionized the Universe escape from galaxies that are above the detection limit of the *Hubble Ultra-Deep Field*. Therefore, the Universe was reionized by relatively bright, vigorously star-forming, compact galaxies.

3 SUMMARY AND CONCLUSION

The fraction of ionizing photons that escapes from galaxies (f_{esc}) is a crucial ingredient in any theory of reionization by galaxies. Observed values of f_{esc} at redshifts $z \lesssim 1$ are small, $f_{\mathrm{esc}} = 1$–2 per cent. This implies that, unless f_{esc} increases rapidly with redshift, reionization was caused by a large population of faint galaxies, below the detection limit of the *HST* and possibly even below that of the *JWST*. The existence of such a population is plausible, given the measured steep faint-end slopes of $z \gtrsim 6$ luminosity functions (e.g. Bouwens et al. 2015a).

The escape fraction of photons from dust-free galaxies is mostly set by the structure of their ISM, since ionizing photons tend to be absorbed close to star-forming region from which they originate. Strong winds, driven by supernovae and massive stars in a star-forming region, are thought to create channels through which photons escape. Such winds tend to be observed when star formation occurs above a given surface density threshold (Heckman 2001), and in the few cases where photons are observed to escape in reasonable fractions of $f_{esc} \gtrsim 20$ per cent, the surface density of star formation is indeed very high (Borthakur et al. 2014; de Barros et al. 2016).

We present a model of reionization that encapsulates these results, by assigning a 20 per cent escape fractions to photons emerging from young star-forming regions with a high value above the $\dot{\Sigma}_{\star,crit} = 0.1$ M$_\odot$ yr^{-1} kpc^{-2} threshold of Heckman (2001), and zero below this threshold. We computed the galaxy-averaged escape fraction as a function of luminosity and redshift by applying this criterion to individual gas particles in the EAGLE simulation, which reproduces the observed star formation rate surface densities as a function of luminosity. We find that luminosity weighted mean value of f_{esc} increases rapidly with redshift, reaching values in the range 5–20 per cent at $z = 6$ for galaxies above the *HST* detection limit, with the brighter galaxies having higher values. Combining this result with the observed luminosity function of galaxies from Bouwens et al. (2015b), we obtain a model that is consistent with the latest constraints on reionization, and on the amplitude of the ionizing background post-reionization. In this model, the *brighter* sources dominate reionization. In particular, we estimate that 50 per cent of the ionizing photons that were emitted before $z = 6$ originated from galaxies above the *Hubble Ultra Deep Field* detection limit. The instantaneous emissivity of those galaxies is $\approx$70 per cent of the total emissivity at that redshift. *JWST* will be able to study these sources in detail.

REFERENCES

Becker G. D., Bolton J. S., 2013, MNRAS, 436, 1023
Bland-Hawthorn J., Maloney P. R., 2001, ApJ, 550, L231
Borthakur S., Heckman T. M., Leitherer C., Overzier R. A., 2014, Science, 346, 216
Bouwens R. J. et al., 2011, ApJ, 737, 90
Bouwens R. J. et al., 2015a, ApJ, 803, 34
Bouwens R. J., Illingworth G. D., Oesch P. A., Caruana J., Holwerda B., Smit R., Wilkins S., 2015b, ApJ, 811, 140
Bridge C. R. et al., 2010, ApJ, 720, 465
Brisbin D., Harwit M., 2012, ApJ, 750, 142
Bruzual G., Charlot S., 2003, MNRAS, 344, 1000
Chen H.-W., Prochaska J. X., Gnedin N. Y., 2007, ApJ, 667, L125
Clarke C., Oey M. S., 2002, MNRAS, 337, 1299
Crain R. A. et al., 2015, MNRAS, 450, 1937
Curtis-Lake E. et al., 2016, MNRAS, 457, 440
de Barros S. et al., 2016, A&A, 585, A51
Ferrara A., Loeb A., 2013, MNRAS, 431, 2826
Fujita A., Martin C. L., Mac Low M.-M., Abel T., 2003, ApJ, 599, 50
Furlong M. et al., 2015a, MNRAS, 450, 4486
Furlong M. et al., 2015b, preprint (arXiv:1510.05645)
Giavalisco M., Steidel C. C., Macchetto F. D., 1996, ApJ, 470, 189
Gnedin N. Y., 2000, ApJ, 535, 530
Grazian A. et al., 2015, A&A, 585, A48
Haardt F., Madau P., 2012, ApJ, 746, 125
Heckman T. M., 2001, in Hibbard J. E., Rupen M., van Gorkom J. H., eds, ASP Conf. Ser. Vol. 240, Gas and Galaxy Evolution. Astron. Soc. Pac., San Francisco, p. 345
Izotov Y. I., Orlitová I., Schaerer D., Thuan T. X., Verhamme A., Guseva N. G., Worseck G., 2016, Nature, 529, 178
Kennicutt R. C., Jr1998, ARA&A, 36, 189
Khaire V., Srianand R., Choudhury T. R., Gaikwad P., 2015, preprint (arxiv:1510.04700)
Kimm T., Cen R., 2014, ApJ, 788, 121
Leitherer C. et al., 1999, ApJS, 123, 3
Loeb A., Barkana R., 2001, ARA&A, 39, 19
Ma X., Kasen D., Hopkins P. F., Faucher-Giguère C.-A., Quataert E., Kereš D., Murray N., 2015, MNRAS, 453, 960
McGreer I. D., Mesinger A., D'Odorico V., 2015, MNRAS, 447, 499
Mitra S., Choudhury T. R., Ferrara A., 2015, MNRAS, 454, L76
Murray N., Ménard B., Thompson T. A., 2011, ApJ, 735, 66
Nestor D. B., Shapley A. E., Kornei K. A., Steidel C. C., Siana B., 2013, ApJ, 765, 47
Paardekooper J.-P., Khochfar S., Dalla Vecchia C., 2015, MNRAS, 451, 2544
Parsa S., Dunlop J. S., McLure R. J., Mortlock A., 2016, MNRAS, 456, 3194
Razoumov A. O., Sommer-Larsen J., 2010, ApJ, 710, 1239
Robertson B. E. et al., 2013, ApJ, 768, 71
Robertson B. E., Ellis R. S., Furlanetto S. R., Dunlop J. S., 2015, ApJ, 802, L19
Rutkowski M. J. et al., 2015, preprint (arxiv:1511.01998)
Scannapieco E., Gray W. J., Pan L., 2012, ApJ, 746, 57
Schaye J., 2004, ApJ, 609, 667
Schaye J., Dalla Vecchia C., 2008, MNRAS, 383, 1210
Schaye J. et al., 2015, MNRAS, 446, 521
Shin M.-S., Trac H., Cen R., 2008, ApJ, 681, 756
Siana B. et al., 2010, ApJ, 723, 241
Vanzella E. et al., 2012, ApJ, 751, 70
Wise J. H., Abel T., 2008, ApJ, 685, 40
Wise J. H., Demchenko V. G., Halicek M. T., Norman M. L., Turk M. J., Abel T., Smith B. D., 2014, MNRAS, 442, 2560
Yajima H., Choi J.-H., Nagamine K., 2011, MNRAS, 412, 411
Zastrow J., Oey M. S., Veilleux S., McDonald M., 2013, ApJ, 779, 76

This paper has been typeset from a TeX/LaTeX file prepared by the author.